UNIVERSITY of CALIFORNIA
SANTA CRUZ

CORE-LEVEL LINE SHAPE ANALYSIS OF $LACOO_3$

A thesis submitted in partial satisfaction of the
requirements for the degree of

BACHELOR OF SCIENCE

in

PHYSICS

by

Eliot M. Paisley

14 June 2009

The thesis of Eliot M. Paisley is approved by:

Professor David P. Belanger
Technical Advisor

Professor Gey-Hong Gweon
Thesis Advisor

Professor David P. Belanger
Chair, Department of Physics

Abstract

Core-level line shape analysis of $LaCoO_3$

by

Eliot M. Paisley

In this thesis we will introduce and explain photoemission spectroscopy and describe the concepts and techniques needed to study the core-level lineshape analysis of lanthanium colbaltite, $LaCoO_3$.

Contents

List of Figures

List of Tables

.

Acknowledgements

I would like to thank Professor Gey-Hong Gweon for having the utmost patience in advising me, and for giving me the opportunity to learn all of the material contained within this thesis under his guidance. I would also like to thank my family, especially my mother, who has supported me thoughout this long journey. And to my live-in psychologist, Jessica Joseph, you are my duck.

1 Motivation

$LaCoO_3$ is a well studied perovskite oxide. This compound is interesting in that when heated to different temperatures, its conductivity changes: it is in a nonmagnetic semiconductor state at low temperatures; a paramagnetic state above 90K; and a metal above 500K.[1] One thing that makes $LaCoO_3$ unique is that as its conductivity changes so does its spin-states. Most of the analysis done on this compound has been performed on its electronic structure, which provides insight into these underlying spin-state(s). [1, 2, 3]. With knowledge of the total spin $\overrightarrow{S}$ as well as the electron's mass, m, charge, q and g-factor g, we can determine the magnetic moment, $\overrightarrow{\mu}$, through the relation $\vec{\mu}_S = g\frac{q}{2m}\,\vec{S}$. This shows that an observed change in magnetism can be directly correlated to spin-state transitions.

One way in which this phenomena is being studied is through the technique of photoemission spectroscopy (PES). Utilizing the core concept of the photoelectric effect, PES gives us a way to calculate and quantify the properties of matter. Great work has been done in the past sixty years to use PES to study the Co^{3+} ion in $LaCoO_3$. [1, 4, 5, 6, 7, 8, 9, 10] However, there is still some dispute as to how to explain the spin-state transitions. A more sophisticated analysis is needed in order to understand this subject with greater certainty.

Over the course of this thesis we will describe the process of photoemission, and explain some of the key concepts that are needed to perform analysis. After taking into consideration some of the more recent advances in the theory of photoemission, we will summarize the current model that will be used for analysis, and then we will explain the necessary calculations and processes.

The idea behind this thesis is to develop a line of theory that will allow us to analyze $LaCoO_3$ using a model that takes into account some of the aforementioned advancements in theory. A subsequent goal of this thesis is to compare and contrast our work with that of our peers, and publish a paper with the most up-to-date analysis of $LaCoO_3$.

2 Initial Considerations

To gain a good understanding of any physical process, it is important to start at the beginning and explain the core concepts first. In this section, we will briefly review the most vital material necessary to understand photoemission spectroscopy and some of the initial associated phenomena.

2.1 Photoelectric Effect

The phenomenon of photoemission was first detected by Heinrich Hertz in 1887[11], but soon became known as the photoelectric effect, according to the interpretation by Albert Einstein[12]. The implementation of this theory to the study of matter has been a grand accomplishment to the advancement of modern physics. Along with the discovery of the quanta of light, the photoelectric effect gives us a theory into how to probe matter at a scale smaller than was previously thought possible. The use of photoemission spectroscopy allows us, as scientists, to create experiments that teach us about the fundamental building blocks of which the world around us is made. With electrons and photons as our subjects, we as controllers of the experiment poke, prod and mold the particles into a configuration with the desired specifics (energy, direction of propagation, polarization) and let loose these energetic beings on paths that will directly impinge on the sample which we desire to study. Typically, the sample is a solid, consisting of a known composition, but properties of its elements are unknown, or poorly understood. Upon impact of the subject particle, energy is transferred from the particle to the sample, and electrons and/or photons escape into the laboratory,

which allows them to be analyzed by apparatus such as spectrometers. In photoelectron spectroscopy, the incoming subject particles are photons, and the ejected particles are electrons. In this thesis we will primarily deal with "core-level photoemission", which implies that the ejected electrons are coming from deep core levels of the sample.

This is the most general idea of photoemission spectroscopy. However, in order to make quantitative predictions, we must consider our physical environment in greater depth.

2.2 The Three-Step Model and The Sudden Approximation

One could, and many have, written entire books on the study of photoelectron spectroscopy and its applications. Writing a thorough and complete guide to the topic is not my aim for this paper. Instead, we will convey a general sense of the phenomena surrounding the physics of the topic, and elaborate when necessary.

Two fundamental ideas now to discuss are known as the 'Three-Step Model', and 'The Sudden Approximation'.

2.2.1 Three-Step Model

In the three-step model the entire photoemission process is broken down into three independent processes. [11]

First The emitted photon is absorbed by the sample and its energy is transferred to individual electrons in the sample, which become excited.

Second Next, the excited electron travels through the sample until it reaches the surface, where it may or may not collide with other particles. Those electrons that *do* collide will suffer an energy loss, and will show on our spectra as a background that can be subtracted off.

Third Finally, the electron escapes the sample through the surface and is detected.

2.2.2 The Sudden Approximation

Loosely stated, in The Sudden Approximation we assume that the eigenstate of an ejected electron will decouple from the system left behind due to the overall process happening very quickly. This is an established theory in itself, and as with the topic of photoemission spectroscopy we are not attempting any type of thorough review.

The essential thing to know is that combining the three-step-model and the sudden approximation gives us a way to theoretically calculate properties of the original sample by measuring values of the ejected electrons and relating them to the 'hole' left behind.

2.3 Multiplet Splitting

In the simplest of cases, the energy of the ejected electron in the photoemission process would have a definite value and could simply be measured. However, there's more to it than that. The first additional consideration goes by the name 'Multiplet Splitting'. Here we will explain this process through a very simple but relevant example.

Consider our sample to be a three-electron atom, typified by lithium. With a ground state electron configuration of $1s^2 2s;\ ^2S$, photoemission from the 1s orbital can yield two distinct final states:

$$Li^+(1s^1 2s;\ ^1S) + e^-$$

$$Li^+(1s^1 2s;\ ^3S) + e^-$$

The difference in final-state angular momenta is a result of the remaining two electrons having spin either antiparallel (^1S state) or parallel (^3S state). This will also result in a difference in energy. The corresponding final-state spin-wavefunctions, using Dirac notation are:

$$^1S \Longrightarrow \psi_{spin} = \frac{1}{\sqrt{2}}(|\uparrow\downarrow\rangle - |\downarrow\uparrow\rangle) \tag{2.1}$$

	Ψ_{total}	ψ_{spin}	$\psi_{spatial}$
^1S	A.S.	A.S.	S.
^3S	A.S.	S.	A.S.

Table 2.1: Summary of Symmetry Arguments in Multiplet Splitting. S. denotes a symmetric state, A.S. denotes an antisymmetric state.

$$^3S \Longrightarrow \psi_{spin} = \frac{1}{\sqrt{2}}(|\uparrow\downarrow\rangle + |\downarrow\uparrow\rangle) \tag{2.2}$$

Now, since electrons are fermions, by Pauli's exclusion principle we know that the overall wavefunction $\Psi = \psi_{spin} * \psi_{spatial}$ must be anti-symmetric. We see that ψ_{spin} is antisymmetric for the ^1S final state, and symmetric for ^3S. Using the mathematical property involving functions that $symmetric * antisymmetric = antisymmetric$, we can conclude that $\psi_{spatial}$ must be symmetric for ^1S, and antisymmetric for ^3S. This is summarized in Table 2.1. Proceeding with a qualitative argument, we now argue that the previous statement results in a energy difference between the two possible final states. For a symmetric spatial wavefunction, the separation distance between particles will be smaller than when compared to that from an antisymmetric spatial wavefunction. This is from the exclusion principle as well. The decrease in separation will produce a more confined system, which results in a higher Couloumb interaction. This increase in Couloumb Repulsion will result in a higher interaction energy. The difference in energy is what is called multiplet splitting.

2.3.1 van Vleck Theorem

From the multiplet splitting defined in the previous section, we can now ask the question "What *is* the energy difference between these two final states?"

John Hasbrouck van Vleck is credited with the appropriately named van Vleck theorem [13] which, for simple situations, gives us the value we are searching for.

$$\Delta E = \frac{2S+1}{2l-1} G^l(s,l) \tag{2.3}$$

The van Vleck theorem applies when we are considering our sample to have an open valance-shell

configuration l^n, with corresponding spin and orbital momenta, and are eliciting photoemission from a filled s shell. S is the total spin pre-photoemission, l the valance shell, and $G^l(s,l)$ the exchange integral. This calculation, which can be made in Hartree-Fock approximations, gives an intensity ratio of multiplets proportional to $\frac{S+1}{S}$

The van Vleck theorem is good for a simple interpretation, but discrepancies arise when the theory is compared to experimental values. Examples are that the measured separation is about 2 times smaller than predicted, and the intensity ratio differs from the short and sweet $\frac{S+1}{S}$.

I will show in subsequent chapters how these discrepancies arise, and illustrate the increasing complexity which we must be able to handle in order to make future predictions.

3 Further Considerations

What was described in Chapter 2 only gives the most rudimentary analysis on the phenomenon of multiplet splitting. Once we consider additional effects, namely that of intrashell correlation and final-state screening, we can analyze the photoemission spectra with a better understanding.

3.1 Intrashell Correlation

An intrashell correlation effect was introduced into the basic multiplet hole theory by Bagus, Freeman, and Sasaki [14] in order to establish better agreement between theory and experiment for the energy separation and the intensity ratio of main and satellite peaks. In the final state after photoemission, excitations were considered such as $\underline{3s}3d^n \rightarrow 3p^2 3d^{n+1}$ or $\underline{3s}3d^n \rightarrow \underline{3s3p^2}3d^{n+2}$ in the 3s photoemission final state. What this effect implies is that in the final state, with the absence of an electron, the remaining electrons may redistribute amongst the available shells.

3.2 Charge-Transfer Splitting - Final State Screening Effect

An additional concept that must be taken into account is the effect of core-hole screening in the final state of photoemission. The Coulomb attraction between a core-hole and localized 3d electrons can cause the neighboring ions (ligands) to try and 'donate' an electron to fill the hole. If this effect is strong, there exist strong "charge transfer satellites" at the higher binding energy side. The electronegativity of the ligand is what determines the intensity and energy position of

these satellites, through what is called the "charge-transfer energy" Δ. Veal and Paulikas [15] were the first to propose an interpretation of the 3s spectra with the final-state screening effect in mind. However, this model is still not without dispute.

A key component for future analysis of $LaCoO_3$ deals with the nature of this screening effect, and so it is important to thoroughly explain it, which we will do through an example. In the 2p photoemission spectra of transition metals the multiplet splitting effect occurs at small energy scales and as such it appears as a mere peak broadening, not as any additional satellites. Since the final state screening effect occurs at the same energy scale for both 2p and 3s photoemission, we may analyze any satellites present in the 2p spectra for evidence of this screening effect.

In Fig. 3.1 we see the 2p photoemission spectra of FeF_2. The bond between the iron and fluorine molecules is ionic in nature, and as such there is less screening in the photoemission process. We see only a small satellite in the region of 6 eV. In an ionic bond, an electron is shared between the two molecules with an intent to reach a noble gas configuration. Generally, in ionic bonding the difference in electronegativity between the two atoms is large. In the case of F and Fe, the difference is 2.15. In comparison, we see in Fig. 3.2 the 2p photoemission spectra of $FeCl_2$. In this case there is a covalent bond between iron and chlorine. For this spectra we can see a much larger satellite located at about 5 eV. This is due to the covalent bond, where the difference in electronegativity is 0.72. These satellites are due to the charge-transfer effect, and clearly demonstrate the role played by the difference in electronegativity.

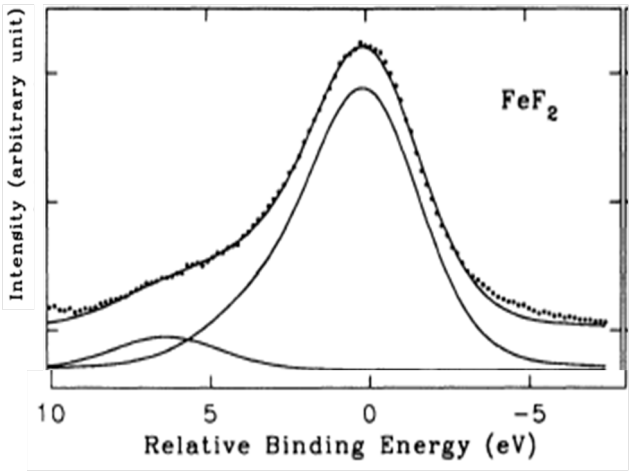

Figure 3.1: FeF_2 2p spectra from Ref[16]. This compound is an ionic structure; note only a small satellite around 6eV.

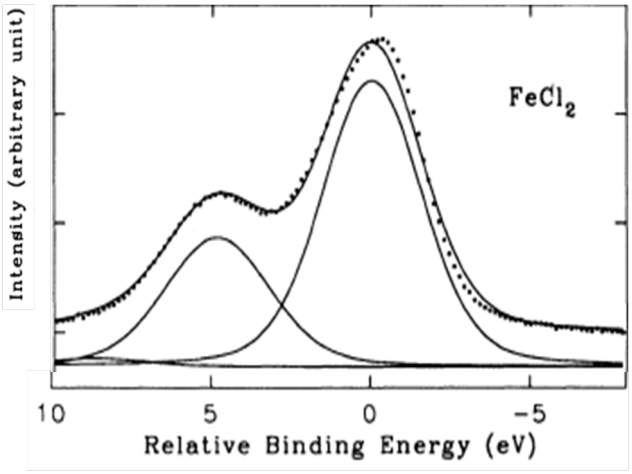

Figure 3.2: $FeCl_2$ 2p spectra from Ref[16]. This compound is a covalent structure; note a much larger satellite around 5eV.

4 Our Calculation Model

Now that we are a bit more sophisticated in our analysis, we need to discuss a calculation method that appropriately accounts for everything. As with most physical processess, the models developed to make calculations are formed and reformed over time, passed through many great minds of science. The practice of theoretically determining the photoemission spectra is no different. We will pick up this theory in a paper published by Park, Ryu, Han, and Oh [17]. After acknowledging many of the (then) current models and discussing the pros and cons of each, Park et. al. describe the theoretical construct to their theory.

They consider the ground state of the system to be a mixture of the configuration $|d^n\rangle (n = 5, 6, 7)$ and the charge-transfer states $|d^{n+1}\underline{L}\rangle, |d^{n+2}\underline{L}^2\rangle, ..., |d^{10}\underline{L}^{10-n}\rangle$. $\underline{L}$ represents the hole in ligand 2p level.

We then define the Hamiltonian of the ground state as a matrix with elements of the following forms: diagonal elements will be $\langle d^{n+q}|H|d^{n+q}\rangle$, where q is defined by the system in question. Off-diagonal elements are mixtures of the states we need to consider. i.e. $\langle d^{n+q}\underline{L}^q|H|d^{n+q+1}\underline{L}^{q+1}\rangle$. At this stage, all other matrix elements are identically zero. We abstain from giving specific parameters to the non-zero matrix elements until the next section when we will discuss the actual model with which we will be working.

After creating our Hamiltonian we can write the ground-state wavefunction as $|\psi_G\rangle = a|d^n\rangle + b|d^{n+1}\underline{L}\rangle + c|d^{n+2}\underline{L}^2\rangle + ... + f|d^{10}\underline{L}^{10-n}\rangle$, with $|a|^2 + |b|^2 + ... + |f|^2 = 1$. Computationally, this wavefunction is found by solving for the eigenvector associated with the lowest eigenvalue. Final-

state wavefunctions for the high-spin and low-spin cases are found in a similar way. The parameters for the corresponding Hamiltonian are adjusted and a matrix is created. The eigenfunctions here represent the wavefunctions for the various satellite peaks that may be created in the photoemission process. The key to this will be to use the sudden approximation for photoionization cross section, reproduced from [17],

$$\rho(\varepsilon_k) \propto \sum |\langle \psi_i | \underline{c} \psi_G \rangle|^2 \delta(\hbar\omega - \varepsilon_k - E_i), \tag{4.1}$$

where $\hbar\omega$ is the photon energy, ε_k the kinetic energy of the photoelectron, and E_i the final-state eigenenergies of the (N-1)-electron system with a core hole. $|\underline{c}\Psi_G$ represents the state obtained by annihilating a core electron in the ground state keeping other orbitals "frozen"[17]. With this equation, we find the intensities of the satellite peaks by calculating the overlap between the final-state wavefunctions with the ground-state wavefunction found from the initial Hamiltonian. The position of the satellite peaks will be the eigenvalues associated to each final-state eigenfunction.

4.1 The Improved Model

In 1993 Gweon, Park and Oh [16] published an update to the photoemission model described above by taking into account both the intrashell correlation effect and core-hole screening. It is this model that we wish to apply to $LaCoO_3$. Let us summarize the model.

The Hamiltonian for the initial state, high-spin final state and low-spin final state will each be slightly different. We will proceed as the paper does and explain the most complex setup, the low-spin final state, and then describe afterwards the adjustments needed to arrive at the initial state and high-spin final state.

The intrashell correlation effect is accounted for in the low-spin final state, as intrashell transitions cannot occur in the high-spin final state for comounds with $n > 5$. While multiple excitations could be influenced by this effect, only the specific case of $\underline{3s}3d^n \longrightarrow \underline{3p}^2 3d^{n+1}$ is considered,

as its contribution is much larger than any other. Two parameters are introduced for this effect, E_{ic}, the energy separation, and V_{ic}, the coupling strength.

Additional parameters are quoted as follows:

"...E_{MHT} is the energy separation given by the multiplet-hole theory. Δ is the charge-transfer energy from the ligand to transition metal ion, U is the d-d Coulomb interaction, Q is the Coulomb interaction between the core hole and d electron, u is the Coulomb interaction between the ligand hole and d electron, and T is the hybridization parameter between the ligand p orbital and the transition-metal d orbital."

The diagonal matrix elements for the hamiltonian have the form:

$\langle \underline{3s}3d^n|H|\underline{3s}3d^n\rangle = E_{MHT}$

$\langle \underline{3s}3d^{n+1}|H|\underline{3s}3d^{n+1}\rangle = E_{MHT} + \Delta - Q_L$

$\langle \underline{3s}3d^{n+2}|H|\underline{3s}3d^{n+2}\rangle = E_{MHT} + 2(\Delta - Q_L) + U$

$\langle \underline{3s}3d^{n+3}|H|\underline{3s}3d^{n+3}\rangle = E_{MHT} + 3(\Delta - Q_L) + 3U$

$\langle \underline{3s}3d^{n+4}|H|\underline{3s}3d^{n+4}\rangle = E_{MHT} + 4(\Delta - Q_L) + 4U$

Etc...

$\langle \underline{3p^2}3d^{n+2}\underline{L}|H|\underline{3p^2}3d^{n+1}\underline{L}\rangle = E_{MHT} + E_{ic}$

$\langle \underline{3p^2}3d^{n+1}\underline{L}|H|\underline{3p^2}3d^{n+1}\underline{L}\rangle = E_{MHT} + E_{ic} + (\Delta - 2Q_{3p} + u) + U$

$\langle \underline{3p^2}3d^{n+3}\underline{L^2}|H|\underline{3p^2}3d^{n+3}\underline{L^2}\rangle = E_{MHT} + E_{ic} + 2(\Delta - 2Q_{3p} + u) + 3U$

While the off-diagonal elements are given by:

$\langle \underline{3s}3d^n|H|\underline{3s}3d^{n+1}\underline{L}\rangle = \sqrt{(10-n)T}$

$\langle \underline{3s}3d^{n+1}\underline{L}|H|\underline{3s}3d^{n+2}\underline{L}^2\rangle = \sqrt{2(9-n)}T$

$\langle \underline{3s}3d^{n+2}\underline{L}^2|H|\underline{3s}3d^{n+3}\underline{L}^3\rangle = \sqrt{3(8-n)}T$

$\langle \underline{3p^2}3d^{n+1}|H|\underline{3p^2}3d^{n+2}\underline{L}\rangle = \sqrt{(9-n)}T$

$\langle \underline{3p^2}3d^{n+2}\underline{L}|H|\underline{3p^2}3d^{n+3}\underline{L}^2\rangle = \sqrt{2(8-n)}T$

$\langle \underline{3s}3d^{n+q}\underline{L}^q|H|\underline{3p^2}3d^{n+q+1}\underline{L}^q\rangle = V_{ic}$

$(q = 0, 1, ..., 9-n)$

The value of n depends on the transition metal being studied; 5 for Mn^{2+}, 6 for Fe^{2+}, 7 for Co^{3+}. q was set equal to u to reduce the number of parameters. If E_{ic} and V_{ic} are set to zero, then the Hamiltonian above becomes the model for the high-spin final state. We can then obtain the initial-state Hamiltonian by setting $Q = 0$ in the high-spin final state. The dimension of each matrix will be $2(10 - n) + 1$ for the 3s low-spin case, and $10 - n + 1$ for the 3s high-spin or 2p final states. As previously explained, the location (energy position) of any existing photoemission peaks are given by the eigenvalues of the Hamiltonian, while the intensities are found from the overlap of the final state eigenvector and the initial state eigenvector.

4.2 Summary

To summarize everything up to now, we present three figures that will illustrate the main points. In Fig. 4.1 we see the 3s photoemission spectra for FeF_2, *without* the intrashell correlation effect or charge-transfer mechanisim accounted for. What we see is a straightforward two-peak spectra which is described nicely by the van Vleck theorem and the multiplet hole theory. In Fig. 4.2 we show the same spectra, but this time we include the intrashell correlation effect. The consequences of this are the peak separation decreasing, by about a factor of 2, and the intensity ratio deviating from the earlier, simpler, picture. Lastly, in Fig. 4.3 we include the charge-transfer mechanism, and see the further complexity that we are dealing with. While the peak separation remains the same as before, we now have additional satellites that must be represented appropriately in the theory. Table 4.1 lists the parameters used to generate these figures. The calculations and plots were performed with Mathematica using the Hamiltonian described in the previous section.

	Δ	U	T	Q_H	Q_L	Q_{3p}	E_{ic}	V_{ic}	E_{MHT}
Fig. 4.1	0	4.0	0	4.5	5.8	5.0	0	0	12.4
Fig. 4.2	0	4.0	0	4.5	5.8	5.0	12.5	10.8	12.4
Fig. 4.3	5.2	4.0	1.4	4.5	5.8	5.0	12.5	10.8	12.4

Table 4.1: Table of parameters used to produce Figures 4.1, 4.2 and 4.3. Values taken from [16].

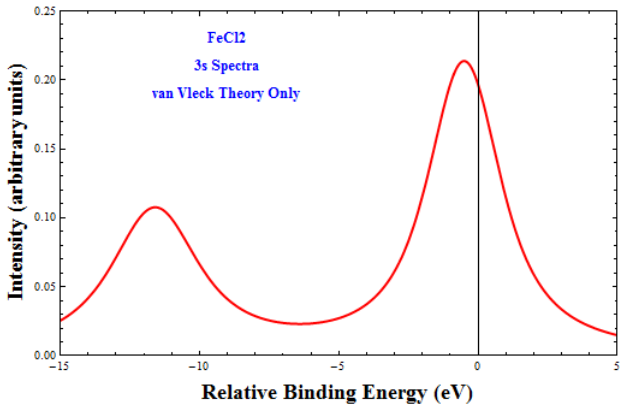

Figure 4.1: $FeCl_2$ 3s Spectra only accounting for the multiplet hole theory predicted by van Vleck.

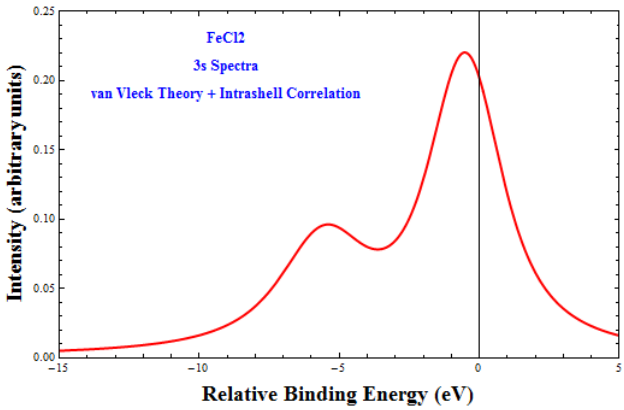

Figure 4.2: $FeCl_2$ 3s Spectra accounting for the van Vleck theory, and intrashell correlation.

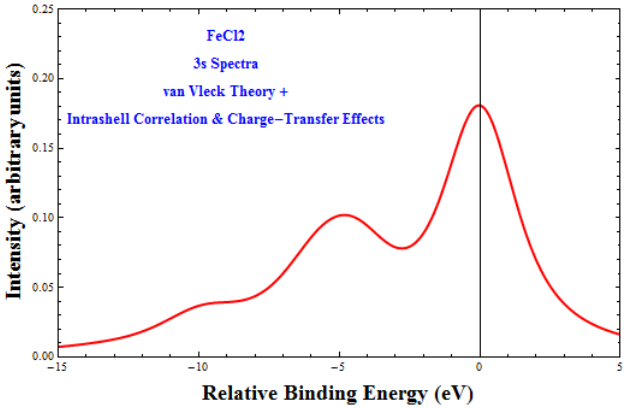

Figure 4.3: $FeCl_2$ 3s Spectra accounting for the van Vleck theory, intrashell correlation, and charge-transfer effect.

5 Current Research - Moving Forward

To continue with the objective of studying the electronic structure of $LaCoO_3$, we must determine the correct parameters to use in the calculation model. To do this we have set forth two goals; first we use previously published data on the 2p spectra of the cobalt ion to gain knowledge of a general range of parameters required, and secondly, we narrow down this range by fitting our calculation model to previously well-established 2p spectra.

Once this has been achieved, we will have a strong grasp on the 2p spectra, and thus the intrashell correlation effect in $LaCoO_3$. After this has been done we can then look to the 3s spectra, and compare and comment on others' published work.

5.1 Previously Published Work

5.1.1 Kinsinger

In 1992 Kinsinger et.al.[18] published a study titled "*Core level exchange splittings in transition metal compounds*". In this paper they obtained a range of parameters by fitting 2p spectra of some transtion metal compunds to a model similar to our own calculation model. Their findings with respect to the cobalt ion are listed in Table 5.1.

	U_{dd}	Δ	U_{cd}	T_i	T_f
CoF_2	4.70	8.60	6.50	1.40	1.85
$CoCl_2$	4.70	4.50	6.50	1.95	1.55
$CoBr_2$	4.70	3.50	6.50	1.35	1.65

Table 5.1: Table of 2p spectra parameters from Ref.[18] which are: U_{dd} (3d electron correlation energy), Δ (charge transfer energy), U_{cd} (core hole valence electron interaction energy) and T_i / T_f (mixing in the initial and final state).

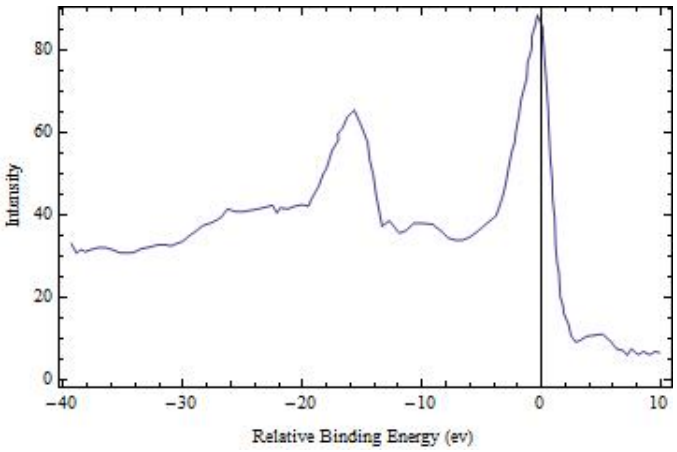

Figure 5.1: Co 2p Spectra from Saitoh et al. Ref[1]

5.1.2 Saitoh

In 1997 Saitoh et al. [1] published an account on the electronic structure of $LaCoO_3$. In this study they perfomed an analysis on the 2p photoemission spectra of the cobalt ion. While their calculation model is different from ours, their published spectra is acknowledged to be well done and thorough. Fig. 5.1 is a reproduction of their spectra after the original graph was digitized and then replotted.

5.2 Moving On...

The search for a correct set of parameters to describe this 2p spectra has begun, but is not yet finished. With a completion date approaching, a thorough analysis is on its way.

6 Conclusion

The study of $LaCoO_3$ and its underlying electronic structure has been a long journey, and it's not over yet. With the theory and analysis of 3s photoemission spectroscopy of transition metal ions now in place, we can perform the appropriate calculations on the cobalt ion to gain a better understaning of this intriguing compound. We have seen the impact that both the intrashell correlation effect and the charge-transfer effect have had on the photoemission spectroscopy theory. An analysis of $LaCoO_3$ that treats both effects on equal ground has not yet been published, and once the path laid out in the past section is finished, we will be able to accomplish just that.

Bibliography

[1] T. Saitoh, T. Mizokawa, A. Fujimori, M. Abbate, Y. Takeda, and M. Takano, Phys. Rev. B **55**, 4257 (1997);

[2] N. Sundaram, Y. Jiang, I.E. Anderson, D.P. Belanger, C.H. Booth, F. Bridges, J.F. Mitchell, Th. Proffen, and H. Zheng, Phys. Rev. Lett. **102**, 026401 (2009);

[3] M. Abbate, J. C. Fuggle, A. Fujimori, L. H. Tjeng, C. T. Chen, R. Potze, G. A. Sawatzky, H. Eisaki, and S. Uchida, Phys. Rev. B **47**, 16124 (1993);

[4] G. Thornton, A. F. Orchard, and C. N. R. Rao, J. Phys. C **9**, 1991 (1976);

[5] B. W. Veal and D. J. Lam, J. Appl. Phys. **49**, 1461 (1978); D. J. Lam, B. W. Veal and D. E. Ellis, Phys. Rev. B **22**, 5730 (1980);

[6] L. Richter, S. D. Bader, and M. B. Brodsky, Phys. Rev. B **22**, 3059 (1980);

[7] J. P. Kemp, D. J. Beal, and P. A. Cox, J. Solid State Chem. **86**, 50 (1990); G. Thornton, I. W. Owen, and G. P. Diakun, J. Phys. Condens. Matter **3**, 417 (1991);

[8] A. Chainani, M. Mathew, and D. D. Sarma, Phys. Rev. B **46**, 9976 (1992);

[9] S. Masuda, M. Aoki, Y. Harada, H. Hirohashi, Y. Watanabe, Y. Sakisaka, and H. Kato, Phys. Rev. Lett. **71**, 4214 (1993);

[10] S. R. Barman and D. D. Sarma, Phys. Rev. B **49**, 13979 (1994);

[11] Stefan Hüfner, *Photoelectron Spectroscopy*, (Springer-Verlag, Germany, 1995);

[12] M. Cardona and L. Ley in *Photoemission in Solids I*, edited by M. Cardona and L. Ley, (Springer-Verlag, New York, 1978), preface.;

[13] J.H. van Vleck, Phys. Rev. **45**, 405 (1934);

[14] P. S. Bagus, A. J. Freeman, and F. Sasaki, Phys. Rev. Lett. **30**, 850 (1973);

[15] B. W. Veal and A. P. Paulikas, Phys. Rev. Lett. **51**, 1995 (1983); B. W. Veal and A. P. Paulikas, Phys. Rev. B **31**, 5399 (1985);

[16] Gey-Hong Gweon, Je-Geun Park, and S.-J. Oh, Phys. Rev. B **48**, 7825 (1993);

[17] Jaehoon Park, Seungoh Ryu, Moon-sup Han, and S.-J. Oh, Phys. Rev. B **37**, 10867 (1988);

[18] V. Kinsinger, R. Zimmermann, S. Hüfner, and P. Steiner, Z. Phys. Condens. Matter **89**, 21 (1992);